iScience

CellPress
OPEN ACCESS

Article

NG2 glia reprogramming induces robust axonal regeneration after spinal cord injury

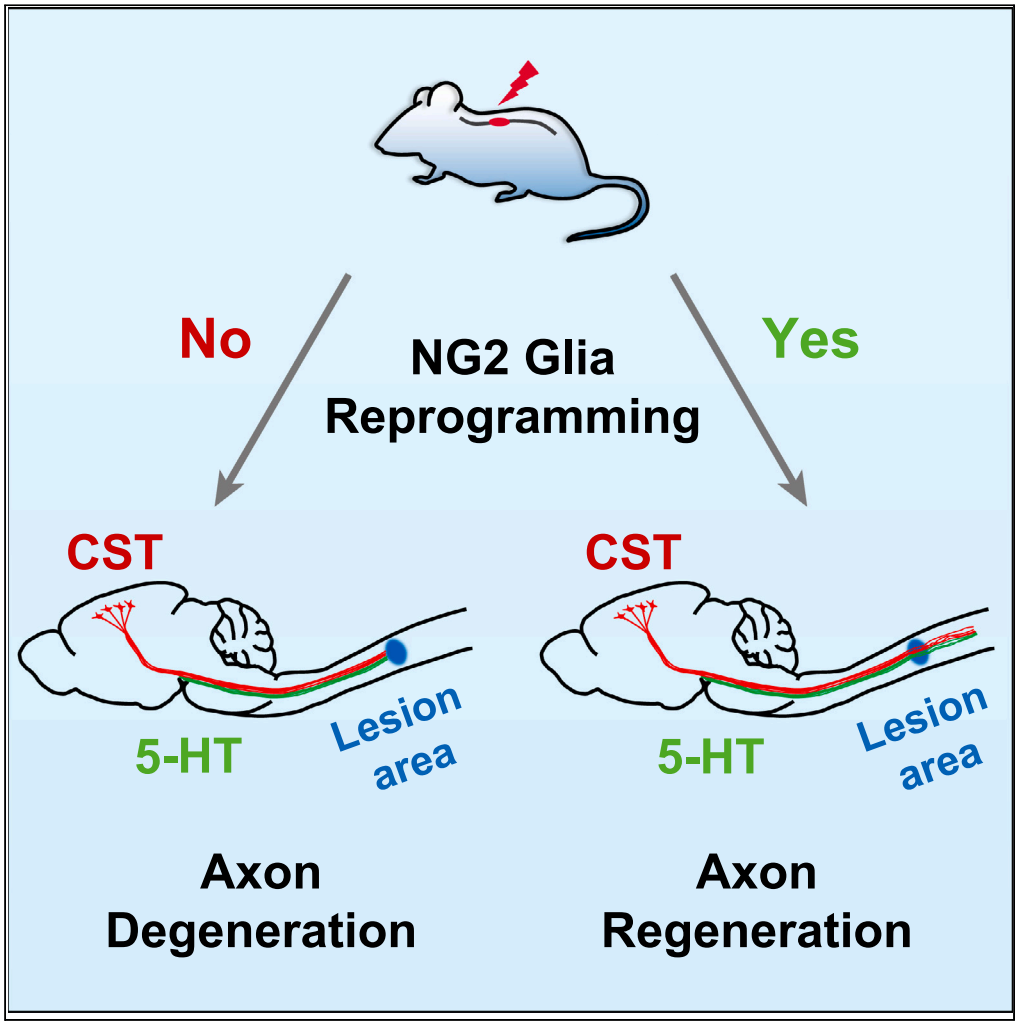

Wenjiao Tai, Xiaolong Du, Chen Chen, Xiao-Ming Xu, Chun-Li Zhang, Wei Wu

chun-li.zhang@utsouthwestern.edu (C.-L.Z.)
wu99@iupui.edu (W.W.)

Highlights

In vivo NG2 glia reprogramming induces robust regeneration of CST axons after SCI

In vivo NG2 glia reprogramming promotes regeneration of 5-HT axons after SCI

Tai et al., iScience *27*, 108895
February 16, 2024
https://doi.org/10.1016/j.isci.2024.108895

iScience

CellPress
OPEN ACCESS

Article

NG2 glia reprogramming induces robust axonal regeneration after spinal cord injury

Wenjiao Tai,[1,3] Xiaolong Du,[2,3] Chen Chen,[2] Xiao-Ming Xu,[2,5] Chun-Li Zhang,[1,*] and Wei Wu[2,4,*]

SUMMARY

Spinal cord injury (SCI) often leads to neuronal loss, axonal degeneration, and behavioral dysfunction. We recently show that *in vivo* reprogramming of NG2 glia produces new neurons, reduces glial scaring, and ultimately leads to improved function after SCI. By examining endogenous neurons, we here unexpectedly uncover that NG2 glia reprogramming also induces robust axonal regeneration of the corticospinal tract and serotonergic neurons. Such reprogramming-induced axonal regeneration may contribute to the reconstruction of neural networks essential for behavioral recovery.

INTRODUCTION

Spinal cord injury (SCI) causes the disruption of neural networks, resulting in significant motor and sensory impairments below the affected area. Unfortunately, the adult spinal cord lacks the ability to naturally generate new neurons, and the inability to regenerate damaged axons further hampers neural repair after injury. Our recent study showed the potential of *in vivo* cell fate reprogramming as a strategy to produce new neurons in the adult mouse spinal cord.[1–3] However, the impact of this reprogramming process on axonal regeneration of endogenous neurons remains unknown.

Failure of axonal regeneration in the adult spinal cord can be attributed to the reduced intrinsic growth ability of neurons as well as the injury-caused inhibitory microenvironment.[4] Enhancing neuronal growth capacity, such as by regulating the PI3K/mTOR signaling pathways, shows promise in promoting axonal regeneration after SCI.[5,6] Similarly, modulating the extrinsic inhibitory microenvironment, such as by degrading the inhibitory chondroitin sulfate proteoglycans (CSPGs) in the lesion scar, also facilitates the regeneration of injured axons across the injury site.[7,8]

A key cellular component of the injury microenvironment is NG2 glia, which are also known as oligodendrocyte precursor cells.[9] They remain largely undifferentiated and play dynamic roles during tissue remodeling and repair after SCI.[9–13] We recently showed that these NG2 glia exhibit latent neurogenic potential in response to SCI and can be further reprogrammed by ectopic SOX2 to become expandable ASCL1$^+$ neural progenitors.[1] By using the *Pdgfra-CreER;Rosa-tdT* mouse lineage-tracing line, we confirmed that adult NG2 glia are the origin of SOX2-induced ASCL1$^+$ progenitors. Furthermore, the reprogrammed cells could also be traced by the thymidine analog BrdU, confirming their proliferative progenitor property.[1] These induced progenitors then generate excitatory and inhibitory neurons that form synaptic connections with local propriospinal neurons and those located in the brain and dorsal root ganglia. Interestingly, SOX2-mediated reprogramming of NG2 glia also changed the microenvironment, indicated by a significant reduction of glial scarring.[1] Such an observation prompted us to examine the same mouse samples that were used in our previous publication for the impact of NG2 glia reprogramming on axonal regeneration surrounding the injury site.

RESULTS

NG2 glia reprogramming induces robust regeneration of CST axons after SCI

We focused on the corticospinal tract (CST), which is known to be the essential pathway for voluntary movement as well as the most challenging pathway for regeneration after injury.[14–17]

We utilized the same previously described mouse samples, in which the SCI was modeled by the 5th cervical vertebra dorsal hemisection (C5-DH).[1] This model of SCI bilaterally eliminates both the dorsal/main and lateral projections of the descending corticospinal tract (CST) such that any axons passing through the lesion site are considered as regenerated. As we previously described,[1] lentivirus encoding the green fluorescence protein (GFP) control, the p75-2 neurotrophic factor, or the SOX2/p75-2 reprogramming factors was delivered to both sides of the lesion one week post injury. At the end of 26 weeks post SCI, we injected AAV8-mCherry as an anterograde tracer into the motor cortex

[1]Department of Molecular Biology and Hamon Center for Regenerative Science and Medicine, University of Texas Southwestern Medical Center, Dallas, TX 75390, USA
[2]Department of Neurological Surgery, Spinal Cord and Brain Injury Research Group, Stark Neuroscience Research Institute, Indiana University School of Medicine, Indianapolis, IN 46202, USA
[3]These authors contributed equally
[4]Lead contact
[5]Deceased
*Correspondence: chun-li.zhang@utsouthwestern.edu (C.-L.Z.), wu99@iupui.edu (W.W.)
https://doi.org/10.1016/j.isci.2024.108895

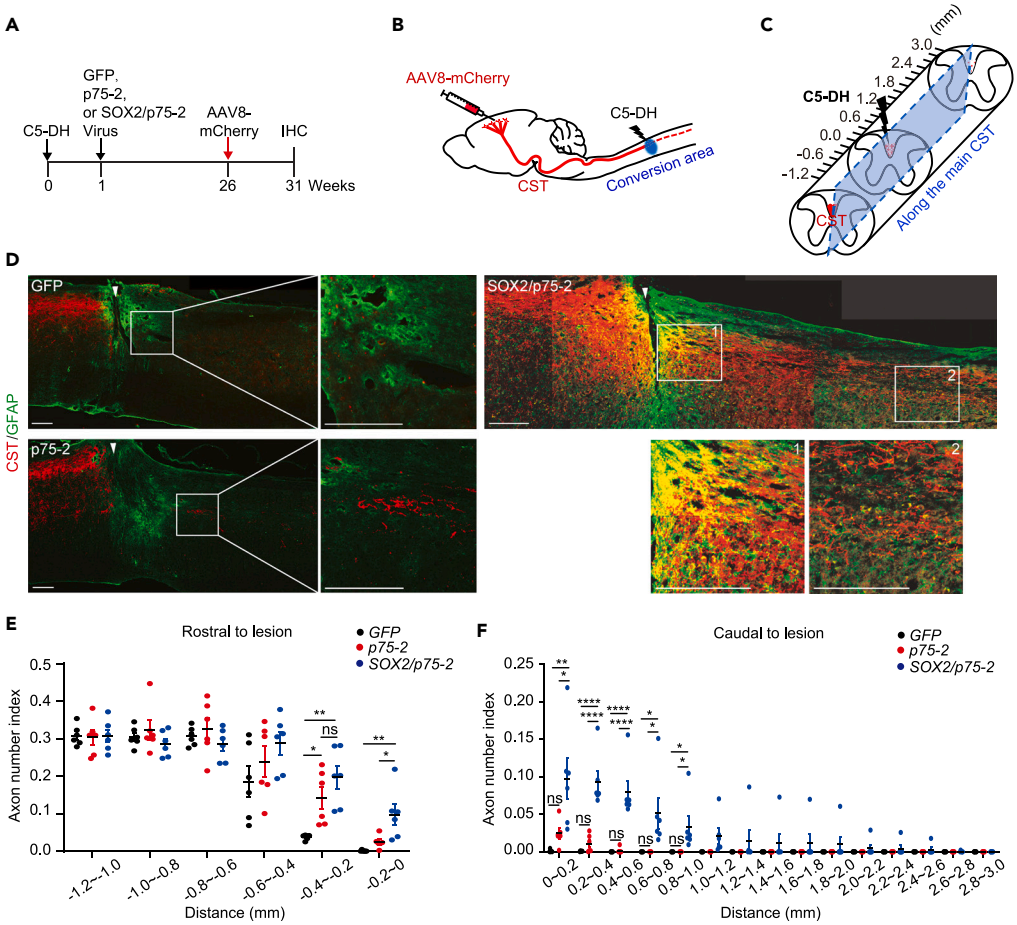

Figure 1. Regeneration of main CST axons induced by NG2 glia reprogramming after SCI

(A) Experimental design. Lentivirus encoding GFP, p75-2 or SOX2/p75-2 was injected into the lesion site rostrally and caudally 1 week post the 5th cervical vertebra dorsal hemisection (C5-DH). Mice were then injected with the anterograde tracer AAV8-mCherry at 26 weeks and analyzed by immunohistochemistry (IHC) at 31 weeks post injury.

(B) Schematic diagram of the injury site and anterograde tracing of the CST axons using AAV8-mCherry virus. The region with virus injections is marked as the conversion area.

(C) Schematic diagram of the spinal cord surrounding the lesion site. The rectangle indicates a sagittal cut through the medial main CST. Axonal densities were measured at both rostral (up to −1.2 mm) and caudal (up to 3.0 mm) sites to the lesion center (0.0 mm).

(D) Confocal images of sagittal sections along the medial main CST. Axons and astrocytes are marked by mCherry and GFAP, respectively. The lesion center is marked by an arrowhead. Enlarged views of the boxed regions are also shown. Scale bars, 200 μm.

(E) Quantification of the medial main CST axon density index at sites rostral to the lesion center (mean ± SEM, *p < 0.05 and **p < 0.01; ns, not significant; one-way ANOVA and Tukey's post hoc multiple comparisons).

(F) Quantification of the medial main CST axon number index at sites caudal to the lesion center (mean ± SEM, *p < 0.05, **p < 0.01, and ****p < 0.0001; ns, not significant; one-way ANOVA and Tukey's post hoc multiple comparisons).

See also Figures S1 and S2.

to label descending CST axons (Figures 1A, 1B, S1A, and S1B). We first examined cross-sections of the spinal cord at the far rostral and caudal level to the lesion site. At the far rostral level medullary pyramids, mCherry-labeled axons were similarly observed among the three treatment groups (Figure S2A), suggesting comparable AAV8-mCherry injections. On the other hand, mCherry-labeled axons were not detected at the lumbar spinal cord among all groups (Figure S2B), supporting a complete transection of the CST in our C5-DH injury model.

We then examined parasagittal sections for mCherry-labeled axons along both the medial main CST (Figure 1C) and those lateral to the main CST (Figure S1C) across the lesion sites, respectively. The GFP group did not show mCherry-labeled CST axons caudal to the lesion core, consistent with the well-established regeneration failure of these axons in the adult spinal cord (Figures 1D and S1D). A closer examination around the lesion site rather showed a retraction of mCherry-labeled axons from the lesion center, a phenomenon known as axon dieback after SCI.[18] This was quantified as a low axon number index at sites rostral to the lesion center (−0.4 to 0 mm; Figures 1E and S1E). For the p75-2 group, a few mCherry-labeled CST axons were detected at the caudal site (Figures 1D and S1D), though the axon number index was not

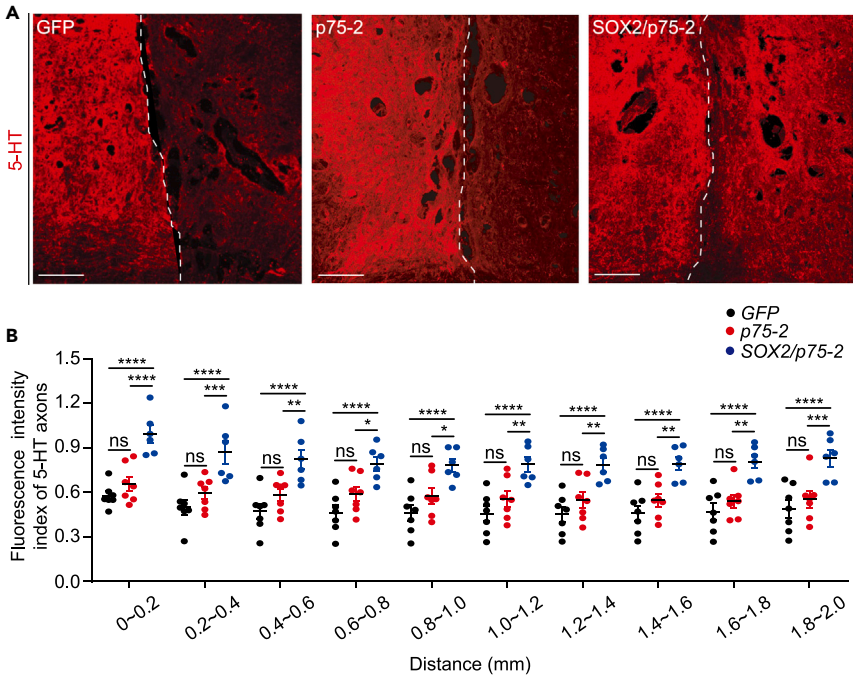

Figure 2. Regeneration of 5-HT axons induced by NG2 glia reprogramming after SCI

(A) Confocal images of 5-HT staining surrounding the lesion center. The dotted line marks the lesion center. Scale bars, 200 μm.

(B) Fluorescence intensity index of 5-HT staining at sites caudal to the lesion center (mean ± SEM, *p < 0.05, **p < 0.01, ***p < 0.001, and ****p < 0.0001; ns, not significant; one-way ANOVA and Tukey's post hoc multiple comparisons).

statistically different from the GFP control (Figures 1F and S1F). Confirming an axon growth-promoting effect of this neurotrophic factor,[19] we did find that the axon number index was higher than the GFP control rostral to the lesion center (−0.4 to −0.2 mm; Figure 1E).

In sharp contrast, the SOX2/p75-2 reprogramming group exhibited very robust regeneration of the mCherry-labeled main CST axons, extending into regions as far as 2.6 mm caudal to the lesion center (Figures 1D–1F). Extensive growth was also observed for axons lateral to the main CST (Figures S1D–S1F). Quantifications confirmed a significantly higher axon number index than either the GFP control or the p75-2 group (Figures 1E, 1F, and S1F). Together, these results clearly showed that SOX2-mediated NG2 glia reprogramming promotes robust regeneration of CST axons after C5-DH.

NG2 glia reprogramming promotes regeneration of 5-HT axons after SCI

We also examined the serotonergic pathway for the effect of NG2 glia reprogramming on axonal regeneration. Serotonin (5-HT) plays an important role in modulating the activity of spinal networks involved in locomotor functions, which is disrupted by SCI, leading to locomotor dysfunction.[20] In contrast to the CST, the 5-HT axons exhibited increased axonal sprouting rostral to the lesion center in all experimental groups (Figure 2A), consistent with the other published observations.[21] When examining the caudal side of the lesion, interestingly, we detected many more 5-HT axons in the SOX2/p75-2 reprogramming group (Figure 2A). Quantitative analysis revealed a significant increase of the fluorescence intensity index within 2.0 mm caudal to lesion border (Figure 2B). Such a result indicates that NG2 glia reprogramming promotes regeneration of 5-HT axons after SCI.

DISCUSSION

In vivo reprograming of resident glial cells is emerging as a regenerative strategy for new neurons in the adult central nervous system.[22–28] For the first time, the results of this study reveal that glia reprogramming also induces robust regeneration of CST axons and 5-HT axons across the lesion after SCI. For decades, the CST and 5-HT pathways have been known to play critical roles in modulating motor function.[20,29] Despite their pivotal roles, adult CST axons and 5-HT axons exhibit limited intrinsic ability to regenerate after SCI.[5,30,31] How does NG2 glia reprogramming lead to enhanced regeneration of these axons?

Both intrinsic and extrinsic pathways are found to control axonal regeneration. For example, transplantation of neural progenitor cells (NPCs) also enables growth of the CST axons into the grafts and beyond the lesion sites.[32] This is largely due to the grafted NPCs reverting the injured CST neurons into an immature transcriptional state.[33] A similar mechanism may be applied to the NG2 reprogramming-initiated axonal regeneration discovered in this study, because many ASCL1$^+$ NPCs and DCX$^+$ immature neurons were induced at the injection sites

during the reprogramming process.[1] These NG2 glia-derived NPCs and immature neurons may remodel in a cell non-autonomous manner the transcriptional programs of CST neurons to enable their intrinsic growths.

The glial scar has been recognized as a critical extrinsic modulator of axonal regeneration. As a major cellular component of the glial scar, NG2 glia rapidly accumulate around the lesion site, leading to increased levels of the NG2 proteoglycan, a key constituent of the inhibitory CSPGs that impede axonal regeneration.[34] NG2 glia play a key role in remodeling the post-SCI tissue for scar formation and their transient early loss but later repopulation leads to axonal growth into the lesion sites.[13] Such a role of NG2 glia is supported by our finding of the reduction of scaring tissues after NG2 glia reprogramming.[1] Of note, NG2 glia reprogramming by SOX2 produces not only new neurons but also an almost equal number of new NG2 glia/oligodendrocytes.[1] These reprogrammed new glial cells may facilitate axonal regrowth as well as their subsequent remyelination.

Together, the results of this study uncover an unexpected biological function of NG2 glia reprogramming *in vivo*. Such reprogramming may have the "kill two birds with one stone" effect on tissue remodeling and regeneration after SCI. Future studies are warranted to systematically dissect the reprogramming-induced regeneration process and develop glia reprogramming as a therapeutic strategy for neural repair.

Limitations of the study

This study reports the initial observation of the effects of *in vivo* glia reprogramming on endogenous neurons. There could be many follow-up investigations. These may include (1) teasing out the underlying molecular mechanisms, (2) conducting multiple injury types on different spinal cord segments along the anterior-posterior axis, (3) performing analyses on multiple time-points post SCI to determine how regenerating axons extend and cross over the lesion site, (4) 3D-tissue analysis with tissue optical clearing and volumetric imaging to unveil the detailed routes and origins of the regenerated axons, (5) mapping the origin of monoaminergic neurons through local injections of a tracer AAV into multiple brain sites (such as the locus coeruleus and the dorsal raphe), and (6) examining the activity of axonal tips with AAV-axoGCaMP and two-photon imaging *in vivo*.[35]

STAR★METHODS

Detailed methods are provided in the online version of this paper and include the following:

SUPPLEMENTAL INFORMATION

Supplemental information can be found online at https://doi.org/10.1016/j.isci.2024.108895.

ACKNOWLEDGMENTS

We thank members of the Zhang and Wu laboratory for discussions and reagents. C.-L.Z. is a W.W. Caruth, Jr. Scholar in Biomedical Research. The work in the Zhang laboratory was supported by the Decherd Foundation, the Texas Alzheimer's Research and Care Consortium (TARCC2020 and TARCC2022), and the NIH (NS099073, NS092616, NS111776, NS117065, and NS088095). The work in the Wu laboratory was supported by the NIH (R01NS103481 and 1R01NS111776) and Indiana Department of Health (ISDH58180).

AUTHOR CONTRIBUTIONS

W.T., W.W., X.-M.X., and C.-L.Z. conceived and designed the experiments. W.T., X.L.D, C.C., and W.W., performed the experiments. W.T., C.-L.Z. and W.W. analyzed data. W.T., C.-L.Z., and W.W. wrote the manuscript. All authors (except for X.-M.X.) reviewed and approved the manuscript.

DECLARATION OF INTERESTS

The authors declare no competing interests.

Received: July 4, 2023
Revised: October 4, 2023
Accepted: January 9, 2024
Published: January 12, 2024

REFERENCES

1. Tai, W., Wu, W., Wang, L.L., Ni, H., Chen, C., Yang, J., Zang, T., Zou, Y., Xu, X.M., and Zhang, C.L. (2021). In vivo reprogramming of NG2 glia enables adult neurogenesis and functional recovery following spinal cord injury. Cell Stem Cell *28*, 923–937.e4.
2. Su, Z., Niu, W., Liu, M.L., Zou, Y., and Zhang, C.L. (2014). In vivo conversion of astrocytes to neurons in the injured adult spinal cord. Nat. Commun. *5*, 3338.
3. Wang, L.L., Su, Z., Tai, W., Zou, Y., Xu, X.M., and Zhang, C.L. (2016). The p53 Pathway Controls SOX2-Mediated Reprogramming in the Adult Mouse Spinal Cord. Cell Rep. *17*, 891–903.
4. Tedeschi, A., and Bradke, F. (2017). Spatial and temporal arrangement of neuronal intrinsic and extrinsic mechanisms controlling axon regeneration. Curr. Opin. Neurobiol. *42*, 118–127.
5. Liu, K., Lu, Y., Lee, J.K., Samara, R., Willenberg, R., Sears-Kraxberger, I., Tedeschi, A., Park, K.K., Jin, D., Cai, B., et al. (2010). PTEN deletion enhances the regenerative ability of adult corticospinal neurons. Nat. Neurosci. *13*, 1075–1081.
6. Al-Ali, H., Ding, Y., Slepak, T., Wu, W., Sun, Y., Martinez, Y., Xu, X.M., Lemmon, V.P., and Bixby, J.L. (2017). The mTOR Substrate S6 Kinase 1 (S6K1) Is a Negative Regulator of Axon Regeneration and a Potential Drug Target for Central Nervous System Injury. J. Neurosci. *37*, 7079–7095.
7. Bradbury, E.J., Moon, L.D.F., Popat, R.J., King, V.R., Bennett, G.S., Patel, P.N., Fawcett, J.W., and McMahon, S.B. (2002). Chondroitinase ABC promotes functional recovery after spinal cord injury. Nature *416*, 636–640.
8. García-Alías, G., Barkhuysen, S., Buckle, M., and Fawcett, J.W. (2009). Chondroitinase ABC treatment opens a window of opportunity for task-specific rehabilitation. Nat. Neurosci. *12*, 1145–1151.
9. Levine, J. (2016). The reactions and role of NG2 glia in spinal cord injury. Brain Res. *1638*, 199–208.
10. Adams, K.L., and Gallo, V. (2018). The diversity and disparity of the glial scar. Nat. Neurosci. *21*, 9–15.
11. Hackett, A.R., and Lee, J.K. (2016). Understanding the NG2 Glial Scar after Spinal Cord Injury. Front. Neurol. *7*, 199.
12. Filous, A.R., Tran, A., Howell, C.J., Busch, S.A., Evans, T.A., Stallcup, W.B., Kang, S.H., Bergles, D.E., Lee, S.I., Levine, J.M., and Silver, J. (2014). Entrapment via synaptic-like connections between NG2 proteoglycan+ cells and dystrophic axons in the lesion plays a role in regeneration failure after spinal cord injury. J. Neurosci. *34*, 16369–16384.
13. Hesp, Z.C., Yoseph, R.Y., Suzuki, R., Jukkola, P., Wilson, C., Nishiyama, A., and McTigue, D.M. (2018). Proliferating NG2-Cell-Dependent Angiogenesis and Scar Formation Alter Axon Growth and Functional Recovery After Spinal Cord Injury in Mice. J. Neurosci. *38*, 1366–1382.
14. Han, Q., Xie, Y., Ordaz, J.D., Huh, A.J., Huang, N., Wu, W., Liu, N., Chamberlain, K.A., Sheng, Z.H., and Xu, X.M. (2020). Restoring Cellular Energetics Promotes Axonal Regeneration and Functional Recovery after Spinal Cord Injury. Cell Metab. *31*, 623–641.e8.
15. Coumans, J.V., Lin, T.T., Dai, H.N., MacArthur, L., McAtee, M., Nash, C., and Bregman, B.S. (2001). Axonal regeneration and functional recovery after complete spinal cord transection in rats by delayed treatment with transplants and neurotrophins. J. Neurosci. *21*, 9334–9344.
16. Mah, K.M., Wu, W., Al-Ali, H., Sun, Y., Han, Q., Ding, Y., Muñoz, M., Xu, X.M., Lemmon, V.P., and Bixby, J.L. (2022). Compounds co-targeting kinases in axon regulatory pathways promote regeneration and behavioral recovery after spinal cord injury in mice. Exp. Neurol. *355*, 114117.
17. Wu, W., Nguyen, T., Ordaz, J.D., Zhang, Y., Liu, N.K., Hu, X., Liu, Y., Ping, X., Han, Q., Wu, X., et al. (2022). Transhemispheric cortex remodeling promotes forelimb recovery after spinal cord injury. JCI insight *7*, e158150.
18. Hill, C.E. (2017). A view from the ending: Axonal dieback and regeneration following. Neurosci. Lett. *652*, 11–24.
19. Enomoto, M., Bunge, M.B., and Tsoulfas, P. (2013). A multifunctional neurotrophin with reduced affinity to p75NTR enhances transplanted Schwann cell survival and axon growth after spinal cord injury. Exp. Neurol. *248*, 170–182.
20. Ghosh, M., and Pearse, D.D. (2014). The role of the serotonergic system in locomotor recovery after spinal cord injury. Front. Neural Circuits *8*, 151.
21. Perrin, F.E., and Noristani, H.N. (2019). Serotonergic mechanisms in spinal cord injury. Exp. Neurol. *318*, 174–191.
22. Bocchi, R., Masserdotti, G., and Götz, M. (2022). Direct neuronal reprogramming: Fast forward from new concepts toward therapeutic approaches. Neuron *110*, 366–393.
23. Vignoles, R., Lentini, C., d'Orange, M., and Heinrich, C. (2019). Direct Lineage Reprogramming for Brain Repair: Breakthroughs and Challenges. Trends Mol. Med. *25*, 897–914.
24. Clifford, T., Finkel, Z., Rodriguez, B., Joseph, A., and Cai, L. (2023). Current Advancements in Spinal Cord Injury Research-Glial Scar Formation and Neural Regeneration. Cells *12*, 853.
25. Zeng, C.W., and Zhang, C.L. (2023). Neuronal regeneration after injury: a new perspective on gene therapy. Front. Neurosci. *17*, 1181816.
26. Tai, W., Xu, X.M., and Zhang, C.L. (2020). Regeneration Through in vivo Cell Fate Reprogramming for Neural Repair. Front. Cell. Neurosci. *14*, 107.
27. Wang, L.-L., and Zhang, C.-L. (2018). Engineering new neurons: in vivo reprogramming in mammalian brain and spinal cord. Cell Tissue Res. *371*, 201–212.
28. Tai, W., and Zhang, C.L. (2023). In vivo cell fate reprogramming for spinal cord repair. Curr. Opin. Genet. Dev. *82*, 102090.
29. Liu, Y., Wang, X., Li, W., Zhang, Q., Li, Y., Zhang, Z., Zhu, J., Chen, B., Williams, P.R., Zhang, Y., et al. (2017). A Sensitized IGF1 Treatment Restores Corticospinal Axon-Dependent Functions. Neuron *95*, 817–833.e4.
30. Curcio, M., and Bradke, F. (2018). Axon Regeneration in the Central Nervous System: Facing the Challenges from the Inside. Annu. Rev. Cell Dev. Biol. *34*, 495–521.
31. Lemon, R.N. (2008). Descending pathways in motor control. Annu. Rev. Neurosci. *31*, 195–218.
32. Kadoya, K., Lu, P., Nguyen, K., Lee-Kubli, C., Kumamaru, H., Yao, L., Knackert, J., Poplawski, G., Dulin, J.N., Strobl, H., et al. (2016). Spinal cord reconstitution with homologous neural grafts enables robust corticospinal regeneration. Nat. Med. *22*, 479–487.
33. Poplawski, G.H.D., Kawaguchi, R., Van Niekerk, E., Lu, P., Mehta, N., Canete, P., Lie, R., Dragatsis, I., Meves, J.M., Zheng, B., et al. (2020). Injured adult neurons regress to an embryonic transcriptional growth state. Nature *581*, 77–82.
34. Tan, A.M., Zhang, W., and Levine, J.M. (2005). NG2: a component of the glial scar that inhibits axon growth. J. Anat. *207*, 717–725.
35. Wu, W., He, S., Wu, J., Chen, C., Li, X., Liu, K., and Qu, J.Y. (2022). Long-term in vivo imaging of mouse spinal cord through an optically cleared intervertebral window. Nat. Commun. *13*, 1959.
36. Zhang, Y.P., Walker, M.J., Shields, L.B.E., Wang, X., Walker, C.L., Xu, X.M., and Shields, C.B. (2013). Controlled cervical laceration injury in mice. J. Vis. Exp. :50030.

STAR★METHODS

KEY RESOURCES TABLE

REAGENT or RESOURCE	SOURCE	IDENTIFIER
Antibodies		
Chicken polyclonal anti-GFAP	Abcam	Cat# ab4674; RRID: AB_304558
Rabbit anti-Serotonin	Sigma-Aldrich	Cat# S5545; RRID: AB_477522
Anti-CD68 antibody, monoclonal	Abcam	Cat# ab31630; RRID: AB_1141557
Alexa Fluor 647 AffiniPure(ab')2 Fragment Donkey Anti-Chicken IgY (IgG)(H+L)	Jackson ImmunoResearch Laboratories	Cat# 703-606-155; RRID: AB_162542
Cy3 AffiniPure F(ab')2 Fragment Donkey Anti-Mouse IgM, u chain specific	Jackson ImmunoResearch Laboratories	715-166-020; RRID: AB_2340815
Goat Anti-Rabbit IgG Antibody, Cy3 conjugate	Millipore Sigma	AP132C; RRID: AB_92489
Bacterial and virus strains		
AAV8-mCherry	LemBix Lab, U Miami	N/A
Experimental models: Organisms/strains		
Mouse: C57BL/6J	The Jackson Laboratory	JAX: 000664; RRID: IMSR_JAX:000664
Recombinant DNA		
LV-hNG2-GFP	Chun-Li Zhang Lab	RRID:Addgene_183910
LV-hNG2-SOX2	Chun-Li Zhang Lab	N/A
LV-p75-2	Pantelis Tsoulfas Lab	RRID: Addgene_73036
Software and algorithms		
ImageJ	NIH	RRID:SCR_003070, https://imagej.net/Fiji
Graphpad Prism	Graphpad	RRID:SCR_002798), https://www.graphpad.com
ZEN	Zeiss	RRID:SCR_013672, https://www.zeiss.com/microscopy/int/products/microscope-software/zen.html
Adobe Photoshop	Adobe	RRID:SCR_014199, https://www.adobe.com/products/photoshop.html
Adobe Illustrator	Adobe	RRID:SCR_010279, https://www.adobe.com/products/illustrator.html
Other		
Louisville Injury System Apparatus	Louisville Impactor System, Louisville, KY	N/A
stereotaxic apparatus	Stoelting Co., Wood Dale, IL	51730
The OLYMPUS FLUOVIEW FV1200 confocal microscope	Olympus Life Science, US	https://www.olympus-lifescience.com/en/laser-scanning/fv1200/

RESOURCE AVAILABILITY

Lead contact

Further information regarding this manuscript and requests should be directed to the lead contact, Dr. Wei Wu (wu99@iupui.edu).

Materials availability

This study did not generate new materials.

Data and code availability

Data: All data are included in the manuscript.

Code: This paper does not report original code.
Any additional information required to reanalyze the data reported in this paper is available from the lead contact upon request.

METHOD DETAILS

Animals

We used the same animal samples that were described in our previous study,[1] Specifically, wild-type C57BL/6J mice (JAX: 000664; RRID: IMSR_JAX:000664) were purchased from the Jackson Laboratory. Adult female mice at 2 months of age and older were used for the experiments. All mice were housed under a controlled temperature and a 12-h light/dark cycle with free access to water and food in the animal facility. Sample sizes were empirically determined. Animal procedures and protocols were approved by the Institutional Animal Care and Use Committee at Indian University School of Medicine or UT Southwestern.

C5-DH spinal cord injuries model and lentivirus injection

As described in our previous study,[1] a laminectomy was conducted to expose the C5 spinal cord after anesthetization (100 mg/kg ketamine, 10 mg/kg xylazine, intraperitoneal injection) and spine stabilization. A transverse durotomy at the interlaminar space was performed using a 30 G needle, which was followed by cutting with a pair of microscissors. The VibraKnife, attached to the Louisville Injury System Apparatus (LISA), was used to cut the spinal cord according to our previously published method.[14,36] The blade, vibrating at 1.2 mm wide, was slowly advanced 1.2 mm ventrally from the dorsal surface of the cord, resulting in a complete transection of the entire dorsal corticospinal tract (dCST) and lateral corticospinal tract (lCST). In this injury model (1.2 mm wide, 1.2 mm depth), any labeled CST axons growing beyond the lesion would be interpreted as coming from cut axons via regeneration from the tips or by regenerative sprouting. One week post injury, a total of 4 stereotaxic viral injections (1-2e9 pfu/ml) were made rostrally and caudally following our previous protocols.[1]

Corticospinal tract tracing

The procedure of tracing the CST axons is similar to our previously published studies.[14,16,17] Specifically, after exposing the skull, bilateral windows (5 mm in length and 2 mm in width) were created with the medial edges of windows 0.5 mm lateral to the bregma. Using a digital stereotaxic injector (Item: 51730, Stoelting Co. USA), 0.5 μl of AAV8-mCherry (5e12 GC/μl) was injected into one of 10 total sites (5 sites/side). The mediolateral (ML) coordination was 1.5 mm lateral to the bregma, the anteroposterior (AP) coordination from the bregma was at -1.0, -0.25, +0.5, +1.25 and +2 mm; dorsoventral (DV) coordination: 0.5 mm from the cortical surface; rate: 0.1 μl/minute. After each injection was completed, the injector tip was left in place for an additional 5 min to adequate penetration of the tracer. Five weeks later, the mice were anesthetized and perfused with 4% paraformaldehyde for detecting CST distribution in the spinal cord.

Immunofluorescence staining

Mice were sacrificed and sequentially perfused with ice-cold phosphate-buffered saline (PBS) and 4% (w/v) paraformaldehyde (PFA) in PBS. Tissues were harvested, post-fixed in 4% PFA overnight, dehydrated in 30% sucrose for 2 days. Serial sagittal or cross cryostat-sections (thickness: 30 μm) were stained with primary antibodies in blocking buffer (3% goat serum or 5% donkey serum in 0.3% PBST) for at least 18 h at 4°C. The primary antibodies were chicken anti-GFAP (1:1000, Abcam, ab4674), rabbit anti-serotonin (5-HT, 1:500, Sigma-Aldrich, S5545) and mouse anti-CD68 (1:500, Abam, ab31630). Detection was accomplished by incubation with Alexa Fluor- or Cy3-conjugated secondary antibodies (Life Technologies/Abcam) diluted in blocking buffer for 2 h at room temperature. The OLYMPUS FLUOVIEW FV1200 confocal microscope was used to visualize the axonal regeneration on the sections (20× and 60×).

Data analysis

To quantify the fiber number index of CST axons, we followed the established protocol[6,14,16] with minor modifications. Briefly, 3-4 sagittal sections from each mouse were analyzed using the ImageJ software. The number of CST axon fragments was counted at defined zones spaced at 0.2 mm apart. The axon number was standardized into Axon Number Index, defined as the ratio of the mCherry-labeled CST axon number at a given zone over the total number of axons of the descending CST on a cross section at the medullary pyramids. The lesion epicenter in the sagittal section was defined as "0" and all other zones were defined as their distance from the lesion center. To quantify the fluorescence intensity index of the 5-HT-positive axons caudal to the lesion site, 3 sagittal sections from each animal were analyzed using ImageJ. In each sagittal section, we first drew a dorsoventral line at the rostral lesion border (0.0 mm) and then vertical lines spaced at 0.2 mm caudal to the dorsoventral line. The axon fluorescence intensity index was presented as a ratio of fluorescence intensity at a specific region versus the intensity at 1.0 mm rostral to the lesion border (-1.0 mm). The averaged axon fluorescence intensity per animal was further processed with the GraphPad software to generate regional density maps at a defined distance from the starting line.

QUANTIFICATION AND STATISTICAL ANALYSIS

All data are presented as mean ± SEM. Statistical analyses were carried out using Prism 7 (Graphpad Software). Comparisons between GFP, p75-2 and SOX2/p75-2 groups were performed by one-way ANOVA and Tukey's post hoc multiple comparisons. A p value < 0.05 was considered significant. Significant differences are indicated by *$p < 0.05$, **$p < 0.01$, ***$p < 0.001$, and ****$p < 0.0001$.